Case Studies in Construction Materials 18 (2023) e01877

Contents lists available at ScienceDirect

Case Studies in Construction Materials

journal homepage: www.elsevier.com/locate/cscm

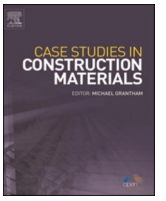

Case study

Evaluation of water loss and stiffness increase in cold recycled mixes during curing

Pablo Orosa *, Ignacio Pérez, Ana R. Pasandín

Universidade da Coruña, Department of Civil Engineering, E. T. S. I. Caminos, Canales y Puertos, Campus de Elviña s/n, 15071 A Coruña, Spain

ARTICLE INFO

Keywords:
Cold recycled mixtures (CRM)
Reclaimed asphalt pavement (RAP)
Bitumen emulsion
Triaxial testing
Nonlinear elastic behavior
Curing

ABSTRACT

Implementing cold solutions is one of the primary efforts in the road sector to counteract CO_2 emissions and climate change. Using cold recycled mixtures (CRM) permits the reuse of up to 100% of reclaimed asphalt pavement (RAP). This research examines how CRM develop their resilient response during the curing process. Using cyclic loading dynamic triaxial (DTx) testing, resilient moduli of CRM made with various proportions of bitumen emulsion were determined. Curing times from 0 days to 18 months were assessed. Binder content and water loss speed proved to be fundamental factors in the evolution of the resilient moduli of the CRM studied. CRM with a binder content of 2.50% exhibited the best short-term response, while those with a binder content of 3.00% showed greater stiffness values over more extended curing. Once water losses stopped, the CRM continued showing changes in stiffness, proving their evolutionary response.

1. Introduction

The current challenge posed by global warming and the need to reduce CO_2 emissions has led to a paradigm shift for many industries, which have had to reconsider many of their working practices [1]. Research and implementation of cold technologies are currently being promoted within the paving sector, thus achieving a degree of decarbonization of its operations. Cold in-place recycling (CIR) and cold central plant recycling (CCPR) are two cold paving techniques that meet these characteristics [2–5]. In addition to being carried out without heating, these techniques reuse the milling from worn-out roads as the solid phase of the new mixtures, providing this material with a second life. The such milled material is commonly referred to as reclaimed asphalt pavement (RAP) [6,7]. The environmental and economic advantages of this type of rehabilitation are diverse [8]; however, it has certain drawbacks, such as the need for a certain curing time to allow the mixtures to develop their mechanical properties.

The need for a curing time is an accepted fact. During this phase, cold asphalt mixtures (CAM) lose their water content and gradually increase their strength [9,10]. However, there is insufficient knowledge and a lack of consensus on this particular stage of cold mixtures, which is why their use is often limited to minor repairs or low-traffic roads. For the laboratory study, it is common to perform accelerated curing procedures of the CAM in an oven, which simulate long periods of natural curing in the field. However, there is no unanimity on these artificial curing procedures. In Spain, it is common to use 3 days at 50 °C for cold recycled mixes (CRM) [11]. However, the standards and recommendations of other countries specify different times and temperatures, ranging from 16 to 72 h and from 40 °C to 60 °C, respectively, whereas other strategies prefer to follow longer curing periods of 7–28 days at room temperature [12].

* Corresponding author.
E-mail addresses: p.orosa@udc.es (P. Orosa), iperez@udc.es (I. Pérez), arodriguezpa@udc.es (A.R. Pasandín).

https://doi.org/10.1016/j.cscm.2023.e01877
Received 22 November 2022; Received in revised form 3 January 2023; Accepted 19 January 2023
Available online 20 January 2023

However, temperature and time are not the only factors affecting the curing of CRM. Another fundamental conditioning factors are the climatic conditions or the construction procedures, in particular, the operations scheduled after the placement and compaction of the CRM layers. The placement of a surface layer on top of the CRM layer, as well as the time programmed before its execution, significantly affect the evolution of the moisture content of the CRM, with clear effects on its mechanical properties. In this regard, Pasetto et al. [13] reported the significant influence of different curing conditions, with different restrictions to water evaporation (free evaporation, partial restriction, or total restriction) during the curing of CBTM on different mechanical properties.

There is a wide range of approaches, but generally, the objective is to reach a constant mass of the studied samples. At this point, it is assumed that the mixtures are stabilized and can be subjected to tests that will inform us of their characteristic properties and optimum binder content. However, this is not entirely true, and it is known that the properties of CAMs are evolutionary and continue to change even after they have cured and lost all their water content [14]. Therefore, it is possible that the binder dosages that were optimal at one time may have changed after longer curing periods. In addition, it should be kept in mind that the equivalences between artificial curing and real curing remain unclear.

2. Aims and scope

The objective of this study was to investigate the evolution with curing of the resilient behavior of CRM prepared with 100% RAP. For this purpose, CRM specimens were prepared with different bitumen emulsion and water contents and were cured at room temperature. Nine curing times, ranging from 0 days to 18 months, were considered to evaluate the short- and long-term properties. Using the same assumptions as previous researchers such as Jenkins, Ebels, or Santagata on the stress-dependent behavior of cold mixes [15–17], the CRM specimens were subjected to cyclic loading dynamic triaxial (DTx) tests to obtain the resilient modulus (*Mr*) at each curing time. The weight losses were recorded for the same specimens subjected to successive DTx tests. As a result, it was possible to correlate the evolution of resilient modulus and water losses and determine the best residual binder dosage at each curing age in terms of resilient modulus.

3. Materials and methods

3.1. Materials

The used RAP was sourced from a local quarry. First, the main properties of the RAP and its recovered bitumen were analyzed. The bitumen content was 4.45%, according to the Spanish standard NLT-164/90 [18], and the maximum specific density was 2425 kg/m^3, obtained according to EN 1097–6 [19]. The recovered bitumen showed 32.15 dmm of penetration grade and 70.20 °C of softening point, obtained according to EN 1426 [20] and EN 1427 [21], respectively.

The size distribution of the RAP batch employed was determined following the standard EN 12697–2 [22]. No particle size adjustments were made to the supplied RAP to simulate the preparation of a CIR-type recycled mixture. Fig. 1 illustrates the RAP particle size distribution, together with the gradation limits of the followed Spanish specification PG-4 [11] and Wirtgen Manual [23], as well as the maximum density line, plotted on the power 0.45 gradation graph.

A paving company provided the used bitumen emulsion, referred to as C60B5-REC according to the European nomenclature [24]. It consisted of a slow-setting cationic emulsion, typically used in Spain in cold recycling works, with 60% of binder content (BC). The basic properties of the bitumen used to prepare the bitumen emulsion were 170 dmm of penetration grade [20] and 36.5 °C of softening point [21].

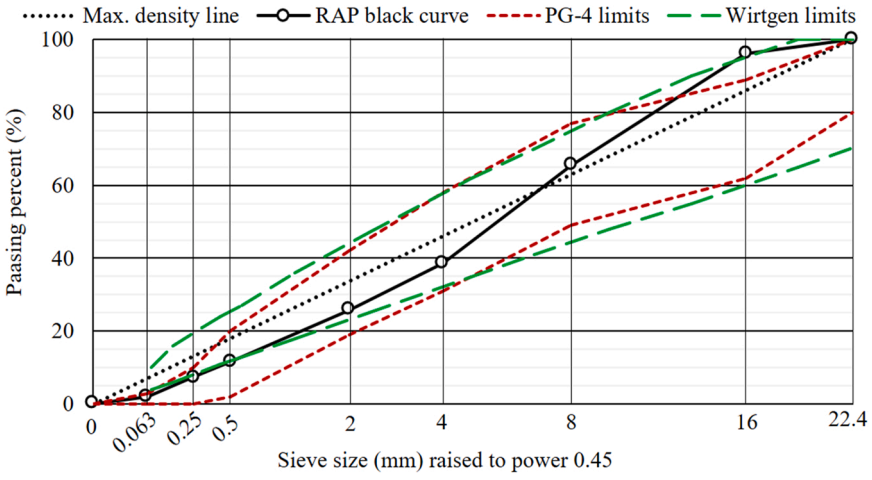

Fig. 1. RAP size distribution (black curve) compared to gradation limits of cold recycling manuals.

3.2. Experimental methodology

3.2.1. Mix design and specimen preparation

The Spanish recycling specifications PG-4 were used to design the mixtures. The solid phase of the mixtures was entirely composed of RAP. According to the PG-4 [11], the BC and the necessary added water contents (AWC) in the mixtures are selected based on the Modified Proctor test (MPT) [25]. Thus, the optimum fluid content (OFC) of the RAP was determined after performing the MPT, corresponding to the moisture value that provided the maximum dry density. Five different BC were selected, ranging from 1.50% to 3.50%, and the corresponding AWC ensured the OFC in all the cases. The followed Spanish PG-4 [11] indicates that the AWC must meet this equation AWC (%) = OFC (%) – 0.5 – BC (%). Table 1 lists the five mixtures studied, the respective BC, AWC, and the corresponding emulsion contents (EC), with three specimens manufactured for each type of mixture.

An automatic mixer was used to mix the components, and a previously verified procedure was followed. First, the entire solid phase was mixed with the corresponding AWC for 60 s to facilitate subsequent coating. After that, the bituminous emulsion was added and mixed for a further 90 s. A gyratory compactor was used following the mixing process. According to EN 12697–31 [26], the gyratory compaction parameters were 0.82 ° of internal rotation angle, 30 rpm rotation speed, and 600 kPa of compaction pressure. Based on PG-4 [11], for the RAP gradation used, 100 mm diameter molds were used, and 100 gyrations were applied, thus ensuring the same compaction energy in all cases.

Triaxial specimens require a height-to-diameter dimensional ratio of 2:1. To produce specimens of 200 mm height, two successively compacted specimens of 100 mm height were stacked one on top of the other. This same production method has already been proven by other researchers [17,27–29] and by the same authors in previous works with triaxial tests [3,30], showing to behave as a single specimen when principal axis stresses are applied.

3.2.2. Curing procedure and measurement of the water loss

All specimens were cured under controlled laboratory conditions (temperature of 22 ± 2 °C and relative humidity of 50 ± 5%). Nine different curing times were considered to study the evolution of stiffness and water loss (0 days, 1 day, 3 days, 7 days, 1 month, 2 months, 6 months, 12 months, and 18 months). A partially sealed curing protocol was followed (Fig. 2a), covering the sides of the specimens using a membrane and allowing evaporation only at the surface [13,31,32]. Since the triaxial resilient modulus tests are non-destructive, the specimens could be tested repeatedly after different curing periods [33,34]. These curing times were selected so that it was possible to analyze both short- and long-term trends.

The first test was performed 4 h after the specimen preparation (we will refer to them as 0 d). The weight of the specimen was always noted before performing the test. Following the test, each specimen was removed from the triaxial chamber, and the weight was again noted to account for the existing losses during testing, due to the axial pressures, especially at early ages when the water content was higher. Then, each specimen was stored to continue curing under ambient conditions (Fig. 2) until the next test date. Repeating this procedure at all curing ages made it possible to evaluate the water losses due to evaporation between curing dates and the water losses during the tests for each mixture.

3.2.3. Evolution of the resilient behavior

The stiffness of cold asphalt mixtures is known to be highly stress-dependent [16,35]. DTx tests following EN 13286–7 [36] were performed to evaluate the resilient behavior of the studied mixtures, determining the resilient modulus (*Mr*). The tests were carried out successively on the same specimens at different curing ages, registering water losses at exact moments. Thus, the evolution of the resilient behavior was evaluated together with the loss of water in the samples, both by evaporation and due to axial pressures during the tests.

Fig. 3 illustrates the equipment used for the triaxial tests. It was used in a removable chamber where the specimens were placed for testing (Fig. 3a). This chamber was connected to a pressurized air system that applied the confining pressure and an independent hydraulic system that controlled the vertical loads. A computer connected to all the systems allowed the overall control and monitoring of the tests and data acquisition. Axial strains were recorded connecting a pair of linear variable strain transducers (LVDTs), which were placed on the top cover of the chamber (Fig. 3b).

The specimens were carefully inserted inside elastic membranes with a diameter slightly larger than the specimens to avoid damage during installation. The specimens were then fixed to porous plates at the top and bottom using O-rings (Fig. 3c). This system allowed for isolating the specimens and applying an adequate confining pressure over the entire lateral surface.

Different constant confining pressures (CCP) with sinusoidal-shaped deviatoric stress were applied during the triaxial tests in accordance with EN 13286–7 [36]. A preliminary conditioning phase was performed before the actual resilient modulus triaxial tests.

Table 1
Binder and water contents selected for the studied CRM.

Mixtures	BC (%)	EC (%)	AWC (%)	OFC (%)
1.5BC	1.50	2.50	3.75	5.75
2.0BC	2.00	3.33	3.25	5.75
2.5BC	2.50	4.17	2.75	5.75
3.0BC	3.00	5.00	2.25	5.75
3.5BC	3.50	5.83	1.75	5.75

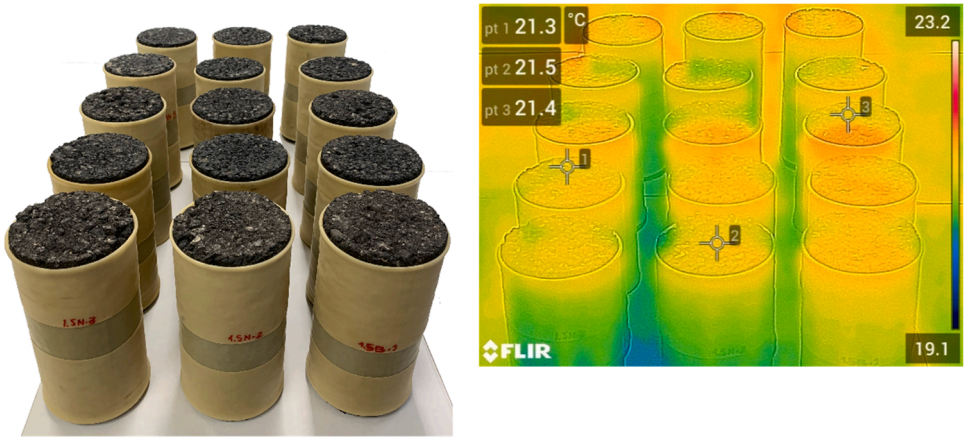

Fig. 2. Storage of the specimens for curing at stable room conditions: (a) Detail of the partially sealed specimens; (b) Thermographic photograph of specimens during curing.

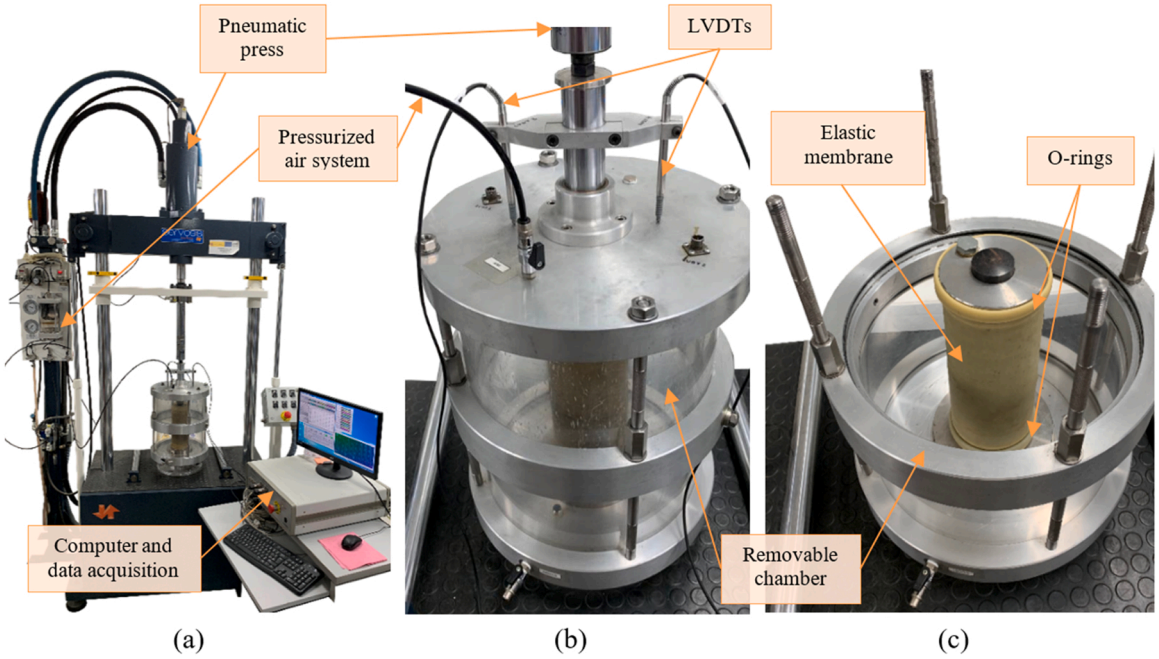

Fig. 3. (a) Overall view of the triaxial equipment; (b) sealed chamber detail with the strain sensors arrangement; (c) detail of the disassembled chamber and sample placement.

During the conditioning phase, a constant confining pressure (σ_3) of 70 kPa was applied, together with a cyclic deviatoric axial stress (σ_d), ranging from 5 to 340 kPa, at a 1 Hz frequency. The conditioning is completed when 20,000 cycles are reached, the permanent deformations rate is less than 10^{-7} per cycle, or the variation of *Mr* is lower than 5 kPa per cycle.

Following the conditioning phase, the resilient modulus triaxial test involved 29 loading series defined in EN 13286–7 [36]. A constant σ_3 and a σ_d with cyclic variation were applied during each loading series, as listed in Table 2. In each loading series, σ_d oscillated between an upper and lower limit for one hundred cycles at a frequency of 1 Hz. The *Mr* was calculated in each cycle using Eq. (1), where σ_d denotes the amplitude of the deviatoric stress, and ε_r denotes the resilient elastic strain. The data acquisition system recorded the result of the last 10 cycles in each loading series.

$$M_r = \sigma_d / \varepsilon_r \quad (1)$$

According to EN 13286–7, the level of stresses applied by these load series corresponds to that experienced by a base course in its upper fiber below a bituminous wearing course of less than 80 mm thickness. Moreover, it indicates that it is possible to define a

Table 2
Series of applied stresses applied during resilient modulus triaxial tests (EN 13286–7).

Loading series	CCP (kPa)	Upper limit of σ_d (kPa)	Lower limit of σ_d (kPa)
1	20	30	20
2		50	35
3		80	50
4		115	70
5	35	50	35
6		80	50
7		115	70
8		150	90
9		200	120
10	50	80	50
11		115	70
12		150	90
13		200	120
14		280	160
15	70	115	70
16		150	90
17		200	120
18		280	160
19		340	200
20	100	150	90
21		200	120
22		280	160
23		340	200
24		400	240
25	150	200	120
26		280	160
27		340	200
28		400	240
29		475	300

characteristic value of *Mr* for the material from the stress-dependent results. This characteristic *Mr* (which we denote as *Mr**) is defined as the modulus of resilience determined for the stress values $p = 250$ kPa and $q = 500$ kPa. These parameters are the mean stress $p = (\sigma_1 + 2\sigma_3)/3$ and deviatoric stress $q = \sigma_d = \sigma_1 - \sigma_3$. In terms of the bulk stress, defined as $\theta = \sigma_1 + 2\sigma_3$, the *Mr** corresponds to the *Mr* when $\theta = 750$ kPa. For each mixture and curing time studied, the value of *Mr** was calculated, thus enabling a simpler comparison between the stiffness results. As an example, Fig. 4 illustrates the *Mr* test result of a specimen of mixture 3.0BC after one month of curing versus the bulk stress, $\theta = \sigma_1 + 2\sigma_3$, and the method of obtaining *Mr** from the test.

3.2.4. *Correlation of Mr* evolution and the mix proportioning*

In recent years there has been a growing usage of tools such as the response surface methodology (RSM) to obtain optimum composite materials designs based on evolutionary mechanical properties [37–39]. From the experimental results of this study, JMP software (SAS Institute, North Carolina, USA) has been used to perform a statistical RSM statistical design. As a result, a second-order model was obtained (Eq. (2)), where *y* is the response variable, β's are the coefficients calculated by the least squares method, and ε is

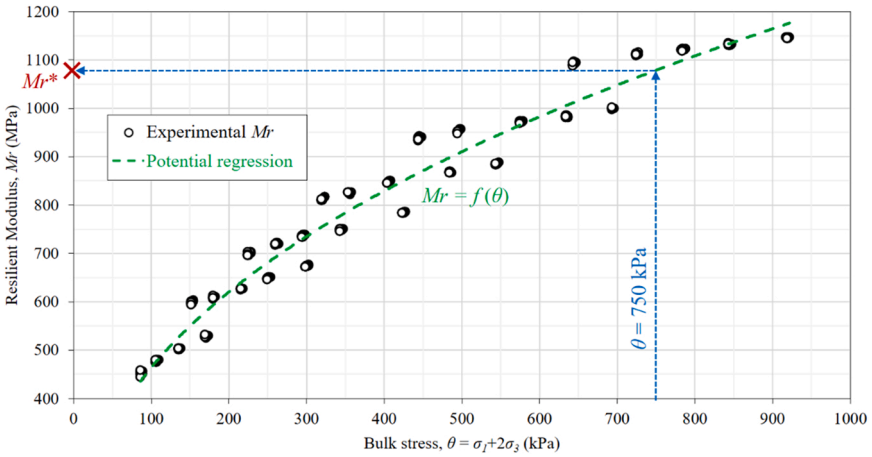

Fig. 4. Determination of the Mr* from the Mr results of a DTx test.

the total error. Additionally, this simulation process facilitated an analysis of variance (ANOVA) that revealed the significance of the studied variables x_i (curing time and binder content) on the Mr^* .

$$y = \beta_0 + \sum_{i=1}^{k} \beta_i x_i + \sum_{i=1}^{k} \beta_{ii} x_i^2 + \sum_i \sum_j \beta_{ii} x_i x_j + \varepsilon \quad (2)$$

4. Results

4.1. Assessment of the water loss of the mixtures

All manufactured specimens were weighed at different times, from the time of manufacture and compaction, and throughout the curing period. All these measurements made it possible to control the weight losses that occurred during the study. Specimen handling was carried out with extreme accuracy, preventing material loss such as aggregates. Thus, two reasons mainly explained these losses: on the one hand, water losses due to evaporation, and on the other hand, water losses during the triaxial tests. These losses for the mixtures studied, corresponding to each curing time, and expressed in per thousand on the initial weight of the specimens, are listed in Table 3 and graphically shown in Fig. 5a. The losses caused by the axial pressures during tests were calculated using the weight differences before and after the tests and were denoted as *testing* losses (Table 3). Whereas *curing* losses correspond to the differences in weight between one curing time and the next, that is, between the weight after the test at one curing time and the weight before the test at the subsequent curing time (Table 3), due to evaporation. Three specimens of each mixture were prepared, and the indicated losses correspond to the mean of the three measurements. Values indicated in Fig. 5a correspond to the sum of both water loss values (*curing* and *testing* losses) for each curing time. Their standard deviations are also listed in Table 3 as a subscript and graphically illustrated in Fig. 5a.

As expected, the highest losses occurred in the first seven days. In particular, the most significant weight losses occurred between days 0 and 1 (row “1 day” in Table 3) and between days 1 and 3 (row “3 days” in Table 3). The 2.5BC mixtures showed the most uniform losses during the first month, with no significant loss peaks. It could be read that this is the binder-water dosage that provides the highest stability of the mixtures. In comparison, mixtures 1.5BC and 2.0BC include a higher AWC, so it is assumed that their losses during these first days were due to higher content of potentially evaporation water. Similar to the mixtures with higher AWC, mixtures with a higher amount of binder (3.00BC and 3.50BC) also showed a slightly higher weight loss than mixture 2.5BC, but not as significant. These two mixtures with higher BC were also visually "darker" due to binder accumulation on the surface, especially mix 3.5BC.

The losses after 1 month of curing, corresponding to the period between 7 days and 1 month (row 1 month in Table 3), were quite similar between the mixes, but 2.5BC still showed the lowest values. However, after 2 months, it is observed that the highest losses

Table 3
Water losses during curing and testing (in ‰of the initial weight of the samples) for the different curing times (corresponding Standard Deviations in subscript).

	Mixtures														
Curing time	1.5BC			2.0BC			2.5BC			3.0BC			3.5BC		
0 days															
testing	3.27	±	0.49	3.17	±	0.28	1.55	±	0.10	3.28	±	0.08	4.57	±	0.44
1 day															
curing	9.07	±	0.19	7.73	±	0.52	5.81	±	2.04	6.40	±	0.32	6.69	±	0.35
testing	1.49	±	0.30	0.85	±	0.34	0.06	±	0.03	0.22	±	0.09	1.01	±	0.91
3 days															
curing	12.10	±	0.96	8.74	±	0.75	4.05	±	0.11	5.38	±	1.19	5.80	±	0.73
testing	0.56	±	0.32	0.36	±	0.13	0.07	±	0.02	0.17	±	0.10	0.22	±	0.09
7 days															
curing	3.05	±	0.13	2.99	±	0.19	2.35	±	0.14	2.93	±	0.27	2.64	±	0.23
testing	0.24	±	0.04	0.28	±	0.06	0.06	±	0.06	0.32	±	0.11	0.39	±	0.05
1 month															
curing	5.56	±	0.08	5.64	±	0.26	3.65	±	0.46	5.73	±	0.44	4.26	±	0.08
testing	0.20	±	0.07	0.21	±	0.06	0.04	±	0.04	0.22	±	0.06	0.22	±	0.08
2 months															
curing	1.61	±	0.48	1.98	±	0.28	1.41	±	0.17	2.35	±	0.17	3.37	±	0.28
testing	0.08	±	0.02	0.07	±	0.05	0.15	±	0.13	0.06	±	0.03	0.04	±	0.02
6 months															
curing	0.79	±	0.06	0.65	±	0.33	0.60	±	0.18	1.89	±	0.56	3.07	±	0.51
testing	0.04	±	0.05	0.02	±	0.06	0.01	±	0.02	0.02	±	0.00	0.08	±	0.17
12 months															
curing	0.01	±	0.02	0.04	±	0.03	0.14	±	0.05	0.06	±	0.06	0.01	±	0.02
testing	0.03	±	0.04	0.02	±	0.01	0.00	±	0.00	0.01	±	0.02	0.00	±	0.00
18 months															
curing	0.01	±	0.03	0.03	±	0.01	0.03	±	0.00	0.05	±	0.05	0.00	±	0.00
testing	0.00	±	0.01	0.01	±	0.01	0.00	±	0.00	0.02	±	0.02	0.00	±	0.00

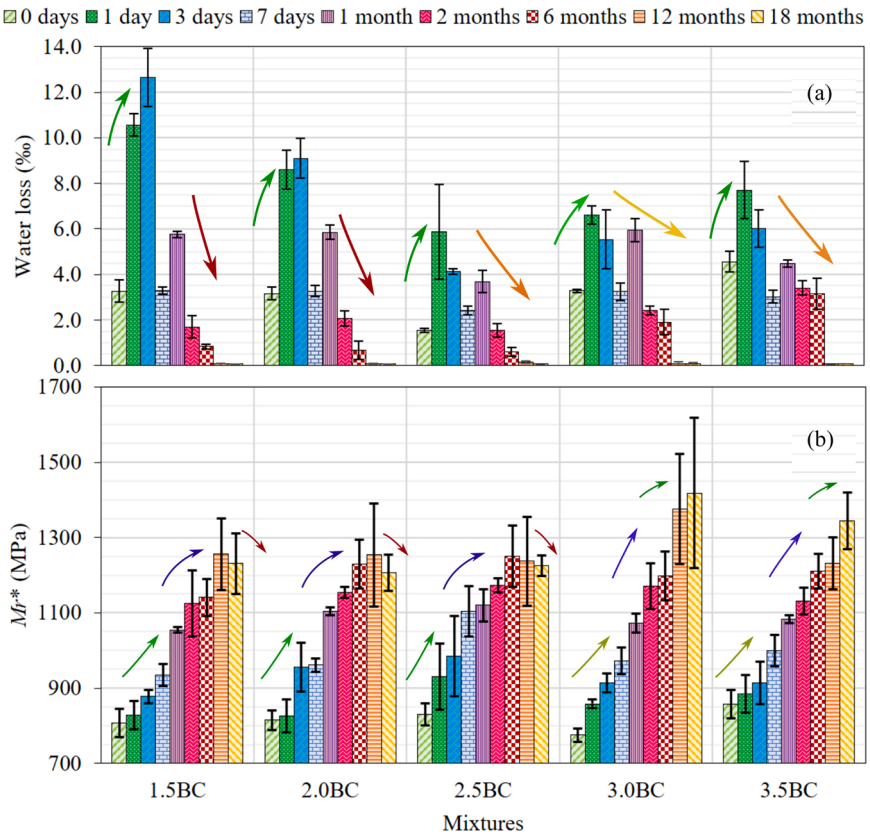

Fig. 5. Water losses and characteristic resilient modulus, Mr^*, of the studied CRM at the different curing times.

were shown in the mixtures with the highest BC. This result could be explained by pore blockage due to excess binder content, producing difficulties for water evaporation in the short term, leading to more prolonged weight loss. After 12 and 18 months, there were still weight variations, but they were less significant, and water evaporations were considered to have ended at this point. The recorded weight differences could be due to minor environmental conditions or small material losses during testing.

4.2. *Evolutionary resilient behavior*

DTx tests were performed successively for each curing time on all the prepared specimens. The stress states listed in Table 2 were applied, and the *Mr* values corresponding to the last 10 cycles of each loading series were obtained. To better compare the results of all the mixes at the different curing times, *Mr** values were obtained as described in Fig. 4 and summarized in Table 4. Since these results are an average of three similar specimens, the standard deviations are also shown as a subscript. Additionally, the *Mr** values were illustrated in Fig. 5b, together with the corresponding water losses in Fig. 5a.

The *Mr** values in Table 4 show a faster evolution in the first 7 days, analogous to the rate of water loss in this period. Mixture 2.5BC

Table 4
Characteristic resilient moduli, *Mr**(in MPa), of the studied CRM at the different curing times (peak values in bold, and corresponding Standard Deviations in subscript).

	Mixtures														
Curing time	1.5BC			2.0BC			2.5BC			3.0BC			3.5BC		
0 days	807.65	±	37.39	814.81	±	26.05	**829.88**	±	29.10	775.19	±	17.92	857.17	±	37.03
1 day	828.11	±	37.11	826.06	±	44.05	**930.99**	±	87.50	858.34	±	12.40	884.80	±	49.63
3 days	877.69	±	17.59	955.63	±	64.46	**984.84**	±	107.46	914.40	±	25.37	914.03	±	57.25
7 days	935.11	±	29.58	961.39	±	17.97	**1103.50**	±	66.55	972.38	±	36.09	999.00	±	41.89
1 month	1054.59	±	7.43	1103.91	±	10.15	**1120.41**	±	42.53	1073.70	±	25.09	1083.32	±	9.99
2 months	1124.61	±	88.27	1154.11	±	14.98	**1173.40**	±	19.24	1170.40	±	60.22	1132.03	±	35.50
6 months	1140.64	±	49.81	1229.30	±	64.82	**1250.50**	±	81.31	1197.57	±	64.44	1210.45	±	45.27
12 months	1256.24	±	94.83	1253.61	±	136.14	1236.77	±	117.51	**1375.38**	±	145.72	1231.62	±	69.14
18 months	1230.88	±	80.81	1205.57	±	47.97	1224.69	±	27.21	**1418.42**	±	200.45	1344.47	±	74.53

showed the highest *Mr** of all the mixtures studied up to the sixth month. It is worth remembering that this mixture showed the most outstanding stability in weight loss, exhibiting the lowest rates. The short-term evolution was very significant in the first 7 days, with the rate decreasing in the following curing times. Thus, the average *Mr** increase between 0 d and 7 d was 21.74%, reaching the maximum increase in the 2.5BC mix with a value of 32.97%. The average increase decreased with the curing time. Thus, between 7 d and 1 month, the average increase in *Mr** was 9.60%; between 1 and 2 months, 5.88%; and between 2 and 6 months, 4.75%.

Interestingly, after 12 months, there was some decrease in the *Mr** values in mixture 2.5BC mixture (which presented the peak values up to now). After 18 months, this reduction continues, and mixtures 1.5BC and 2.0BC join this decreasing trend. In this regard, the relationship between water losses and *Mr** growth is more evident considering both graphs in Fig. 5. These are precisely the three mixtures (1.5BC, 2.0BC, and 2.5BC) that show the most rapid growth in water losses and a more pronounced drop after the first 7 days of curing. Experts such as Needham [33] or Pasandín et al. [40] reported that although resilient modulus tests are non-destructive, some internal damage or micro-deterioration may occur due to successive repetition of such tests on the same specimens over time. Particularly CRM specimens with the lowest binder content are the most prone to exhibit permanent deformations [16]. Furthermore, the faster water loss could be related to the loss of resilient modulus after a certain curing time.

In contrast, mixtures with higher binder content (3.0BC and 3.5BC) showed a less pronounced growth in water losses and a more steady decline, as seen in Fig. 5a. These more sustained water losses could be related to a more consistent growth in the *Mr** , which did not show any decrease after 18 months. These higher long-term stiffness values could also be expected due to the higher binder content and its aging and stiffening. Such binder aging could lead to increased stiffness of the CRM even after the curing period, especially those with higher binder content [14]. After 12 and 18 months, the peak average *Mr** values were exhibited by the mixture 3.0BC (Fig. 5b).

Given the observed trend of the results, Fig. 6 shows the cumulative increase of *Mr** versus the respective cumulative water losses of the studied mixtures to analyze the relationship between these two measured variables. Each marker refers to the average of 3 specimens' results at the successive studied curing time. The faster *Mr** increase of the 2.5BC mixture in the short term is noticeable, while 3.0BC exhibited the highest *Mr** values in the long term. Mixture 1.5BC showed the highest water losses and generally the lowest *Mr** values.

Interestingly, the relationship is quite linear for the initial curing times, as described in previous research [3]. However, *Mr** continues to increase when water losses cease, and at this point, it is observed that for more extended periods, the growth trend resembles an exponential pattern for all the studied mixtures (Fig. 6). From this result, it can be concluded that the improvement in stiffness and the resilient mechanical behavior of CRM is undoubtedly related to water loss during curing. However, the resilient behavior of the studied CRM showed maturation and evolution beyond the end of the curing period. Furthermore, the optimum binder dosage was not the same for all ages. Mixture 2.5BC showed the best performance in the short-term with the fastest *Mr** evolution, but mixture 3.0BC showed the highest *Mr** values for more advanced times and continued the increasing trend.

Analyzing this graph in Fig. 6, it is noticeable that the 2.5BC and 3.0BC mixes appear more to the left; therefore, they are the ones with the fastest evolution of *Mr** with the loss of water (greater slope). Consequently, and in addition to the conclusions from Fig. 5, it can be stated that a residual binder dosage between 2.5% and 3.0% returned the best results regarding stiffness evolution for the studied CRM. The CRM with a 3.0% residual binder content was optimal since it showed the highest *Mr** values and no decrement in the long term.

4.3. Correlation of Mr* evolution and the mix proportioning

The experimental results made it possible to use the RSM to obtain a second-order model of *Mr** , in MPa, as a function of the curing time (*T*), in days, and binder content (*BC*), in percentage, and it is shown in Eq. (3).

$$Mr^* = 698.19 + 1.84 \cdot T + 192.41 \cdot BC - 0.003 \cdot T^2 - 36.36 \cdot BC^2 + 0.1 \cdot T \cdot BC \quad (3)$$

The ANOVA analysis evaluated the significance of the variables studied, and the p-values obtained are summarized in Table 5. It was observed that the most influential variable, as expected, is the curing time (*T* and T^2), showing the lowest p-values. The binder content variable (*BC*) showed a p-value of 0.11041, with a still relevant weight in the model, while the significance was lower in the case of its cross variables ($T \cdot BC$, and BC^2), with higher p-values according to the ANOVA analysis.

Finally, Fig. 7 shows the correlation between experimental *Mr** values and those predicted by the model from Eq. (3), showing an acceptable fit, with a total error below 20% in all cases and below 10% in most of them. For the mix design of the studied CRMs, the AWC used depended on the BC to ensure the OFC, and therefore the variable water content was not included in the model. However, a broader study where additional water contents are investigated for the same binder content is found interesting in order to feed a complete predictive model and to be able to draw broader conclusions.

5. Conclusions

In this study, the resilient moduli of CRM were obtained by performing DTx tests. The CRM were prepared with a gyratory compactor using a different binder and water contents and were cured under room conditions. The triaxial tests were successively repeated at different curing times (0 d, 1 d, 3 d, 7 d, 1 month, 2 months, 6 months, 12 months and 18 months) and the water loss over time was registered. The results were correlated and the evolutionary nature of the resilient behavior of the CRM was shown. Conclusions drawn from the study include the following:

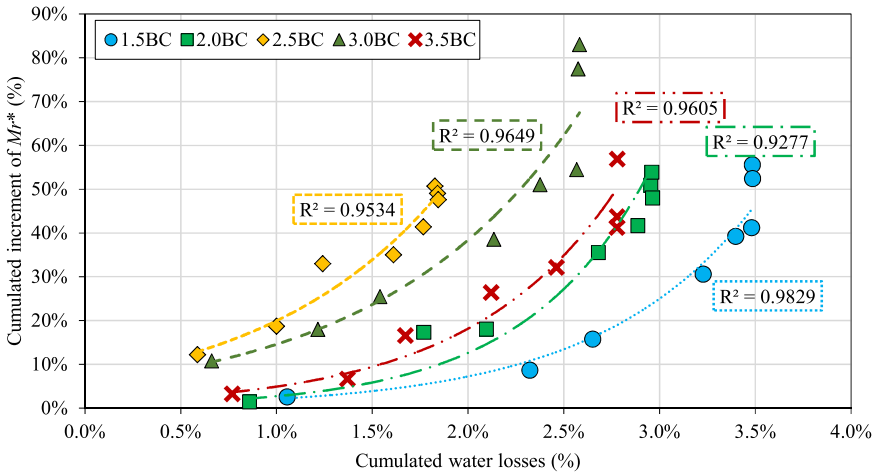

Fig. 6. Relationship between the cumulative increase in *Mr** and the cumulative water losses.

Table 5
ANOVA analysis results (Mr*, response variable).

Variables	P-values
T	0.00000
BC	0.11041
T^2	0.00001
BC^2	0.24060
T·BC	0.32720

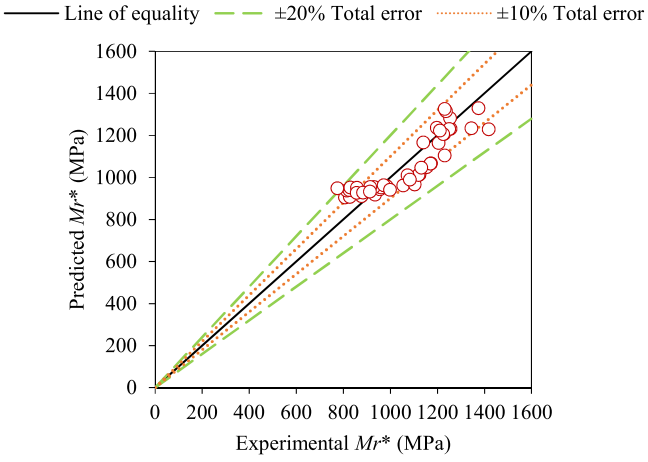

Fig. 7. Predicted versus measured characteristic resilient modulus and total error limits.

- Water losses due to evaporation during curing and those occurring during triaxial tests due to the axial pressures were recorded. Water losses in the short term were more meaningful. After one month, the losses stabilized, and after 6 months, they were less significant.
- Mixture 2.5BC showed the most stable water losses. Mixtures with less binder content and more added water showed higher water losses in the first few days, while those with more binder content and lower added water showed more sustained losses over extended periods.
- In the short term, the *Mr** of mixture 2.5BC were the highest, but after 12 months they stabilized and even decreased. Mixtures with 1.5BC and 2.0BC also decreased the *Mr** values after 18 months. This decrease in *Mr** was associated with the possibility of micro-deterioration after successive non-destructive tests, especially in the CRM with a lower binder content (more susceptible to permanent deformations).

- Mixtures with 3.0BC and 3.5BC steadily increased their *Mr** values even up to the 18 months studied. After 12 months, mixture 3.0BC showed the highest *Mr** values. This sustained growth over time was associated with a more constant water loss throughout curing, which was not as fast in the short term, and remained more stable in the long term compared to the other CRM studied. In addition, beyond the end of the curing period, aging and stiffening of the binder could lead to an increase in *Mr** , especially in these CRM with higher binder content.
- The increases in *Mr** and the water loss showed a reasonably linear relationship in the early curing stages. When water loss was less significant, the correlation was more similar to an exponential form. The resilient behavior was considered evolutionary beyond the end of the curing period.
- The ANOVA statistical analysis showed that the most significant variable in the evolution of the resilient modulus was the curing time. In addition, the binder content variable also showed a considerable degree of significance.

While dynamic triaxial tests are considered non-destructive, it is possible that imperceptible micro-deterioration may occur inside the CRM specimens after multiple repetitions. This damage may be the reason for the long-term reduction of *Mr*. Such reductions occurred precisely in the CRM with lower binder contents, which are more susceptible to permanent deformations and damages. However, damage to CRM also occurs in the actual pavement, mainly due to traffic loading. Therefore, such an increasing trend in *Mr* during curing, stabilization, and a slight decrease in the long term is an expected trend for a CRM in the field. A study of a more extended curing period could be interesting to see if the reported trends continue. Regardless of the total fluid content, which was constant among the CRM studied, the results of this study highlighted the substantial influence of the water content and its evaporation rate. In this sense, it raises interest in investigating the water content resulting in better mixing and compaction of CRM and the evolution of its mechanical properties in the short and long term.

Declaration of Competing Interest

The authors declare that they have no known competing financial interests or personal relationships that could have appeared to influence the work reported in this paper.

Data Availability

Data will be made available on request.

Acknowledgments

The authors would like to acknowledge the funding for the project *BIA2016–80317-R/AEI/10.13039/501100011033* from the Spanish Ministry of Science and Innovation, with an associated pre-doctoral scholarship for the training of research workers (FPI) *BES-2017-079633*. The authors would also like to express their sincere gratitude to ARIAS INFRAESTRUCTURAS and ECOASFALT for their generous donation of RAP and bitumen emulsion, respectively, for the present research. An special acknowledgement to the Universidade da Coruña/ CISUG for funding part of the Elsevier's open acces charge. Finally, the corresponding author expresses his gratitude to Natalia Pérez-Barge, and Jorge del Valle Corte for their help and support during the laboratory works, and to Marina G. López-Arias for her help with the analysis of the results.

References

[1] F.D.B. Albuquerque, M.A. Maraqa, R. Chowdhury, T. Mauga, M. Alzard, Greenhouse gas emissions associated with road transport projects: Current status, benchmarking, and assessment tools, Transp. Res. Procedia 48 (2020) 2018–2030, https://doi.org/10.1016/j.trpro.2020.08.261.
[2] A. Saidi, A. Ali, Y. Mehta, B.C. Cox, W. Lein, Evaluation of laboratory and field performance of cold in-place recycling (CIR) asphalt mixtures, Proc. RILEM Int. Symp. Bitum. Mater. (2022) 803–809, https://doi.org/10.1007/978-3-030-46455-4_102.
[3] P. Orosa, I. Pérez, A.R. Pasandín, Short-term resilient behaviour and its evolution with curing in cold in-place recycled asphalt mixtures, Constr. Build. Mater. 323 (2022), 126559, https://doi.org/10.1016/j.conbuildmat.2022.126559.
[4] S. Jain, B. Singh, Cold mix asphalt: an overview, J. Clean. Prod. 280 (2021), 124378, https://doi.org/10.1016/j.jclepro.2020.124378.
[5] B.K. Diefenderfer, D.H. Timm, B.F. Bowers, Structural Study of Cold Central Plant Recycling Sections at the National Center for Asphalt Technology (NCAT) Test Track: Phase II, Virginia. Dept. of Transportation, 2019.
[6] S. Magar, F. Xiao, D. Singh, B. Showkat, Applications of reclaimed asphalt pavement in India – a review, J. Clean. Prod. 335 (2022), 130221, https://doi.org/10.1016/j.jclepro.2021.130221.
[7] F. Xiao, N. Su, S. Yao, S. Amirkhanian, J. Wang, Performance grades, environmental and economic investigations of reclaimed asphalt pavement materials, J. Clean. Prod. 211 (2019) 1299–1312, https://doi.org/10.1016/j.jclepro.2018.11.126.
[8] A. Pakes, T. Edil, M. Sanger, R. Olley, T. Klink, Environmental benefits of cold-in-place recycling, Transp. Res. Rec. J. Transp. Res. Board. 2672 (2018) 11–19, https://doi.org/10.1177/0361198118758691.
[9] A. Graziani, C. Iafelice, S. Raschia, D. Perraton, A. Carter, A procedure for characterizing the curing process of cold recycled bitumen emulsion mixtures, Constr. Build. Mater. 173 (2018) 754–762, https://doi.org/10.1016/j.conbuildmat.2018.04.091.
[10] G. Ferrotti, A. Grilli, C. Mignini, A. Graziani, Materials Comparing the Field and Laboratory Curing Behaviour of Cold Recycled Asphalt Mixtures for Binder Courses, (n.d.). https://doi.org/10.3390/ma13214697.
[11] Spanish Ministry of Development, PG-4, Recycling of bituminous pavements and roadways, Circ. Order 40/2017 (2017).
[12] P. Orosa, A.R. Pasandín, I. Pérez, Assessment of two laboratory design methods for CIR mixtures with bitumen emulsion based on static and gyratory compaction, Constr. Build. Mater. 265 (2020), https://doi.org/10.1016/j.conbuildmat.2020.120667.

[13] M. Pasetto, E. Pasquini, A. Baliello, S. Raschia, A. Rahmanbeiki, A. Carter, D. Perraton, F. Preti, B.C.S. Gouveia, G. Tebaldi, A. Grilli, E.V. Dave, Influence of curing on the mechanical properties of cement-bitumen treated materials using foamed bitumen: an interlaboratory test program, Lect. Notes Civ. Eng. 76 (2020) 55–65, https://doi.org/10.1007/978-3-030-48679-2_6/TABLES/5.
[14] B. Gómez-Meijide, I. Pérez, A.R. Pasandín, Recycled construction and demolition waste in cold asphalt mixtures: evolutionary properties, J. Clean. Prod. 112 (2016) 588–598, https://doi.org/10.1016/j.jclepro.2015.08.038.
[15] K.J. Jenkins, F.M. Long, L.-J. Ebels, Foamed bitumen mixes = shear performance? Int. J. Pavement Eng. 8 (2007) 85–98, https://doi.org/10.1080/10298430601149718.
[16] L.-J. Ebels, Characterisation of Material Properties and Behaviour of Cold Bituminous Mixtures for Road Pavements. Ph.D. Dissertation. Stellenbosch University, 2008.
[17] E. Santagata, G. Chiappinelli, P.P. Riviera, O. Baglieri, Triaxial testing for the short term evaluation of cold-recycled bituminous mixtures, Road. Mater. Pavement Des. 11 (2010) 123–147, https://doi.org/10.1080/14680629.2010.9690263.
[18] Ministry of Public Works and Transport, NLT standards. NLT–164/90. Binder content in bituminous mixtures. Road tests. General Directorate for Roads, Madrid, Spain, 1990.
[19] AENOR (Spanish Association for Standardisation and Certification), UNE - EN 1097–6. Tests to determine the mechanical and physical properties of aggregates. Part 6: Determination of particle density and water absorption., In Spanish, Madrid, 2006.
[20] AENOR (Spanish Association for Standardisation and Certification), UNE - EN 1426. Bitumen and bituminous binders. Determination of needle penetration., In Spanish, Madrid, 2015.
[21] AENOR (Spanish Association for Standardisation and Certification), UNE - EN 1427. Bitumen and bituminous binders. Determination of the softening point. Ring and Ball method., In Spanish, Madrid, 2015.
[22] AENOR (Spanish Association for Standardisation and Certification), UNE - EN 2 12697–2. Bituminous mixtures. Test methods. Part 2: Determination of particle size 3 distribution., In Spanish, Madrid, Spain, 2015.
[23] Wirtgen GmbH, Wirtgen Cold Recycling Technology, Wirtgen Cold Recycl. Technol. (2012) 367.
[24] AENOR (Spanish Association for Standardisation and Certification), UNE - EN 13808. Bitumen and bituminous binders. Framework for specifying cationic bituminous emulsions., In Spanish, Madrid, Spain, 2020.
[25] AENOR (Spanish Association for Standardisation and Certification), UNE - EN 103–501-94. Geotechnics. Compaction test. Modified Proctor., In Spanish, Madrid, Spain, 1994.
[26] AENOR (Spanish Association for Standardisation and Certification), UNE - EN 12697–31. Bituminous mixtures. Test methods for hot bituminous mixtures. Part 31: Specimen preparation by gyratory compactor, in Spanish, Madrid, 2008.
[27] B. Gómez-Meijide, I. Pérez, Nonlinear elastic behavior of bitumen emulsion-stabilized materials with C&D waste aggregates, Constr. Build. Mater. 98 (2015) 853–863, https://doi.org/10.1016/j.conbuildmat.2015.07.004.
[28] T. Yun, Y.Richard Kim, Viscoelastoplastic modeling of the behavior of hot mix asphalt in compression, KSCE J. Civ. Eng. 17 (2013) 1323–1332, https://doi.org/10.1007/s12205-013-0352-7.
[29] W. Kim, J. Labuz, Resilient modulus and strength of base course with recycled bituminous material. Technical Report, 2007.
[30] P. Orosa, I. Pérez, A.R. Pasandín, Evaluation of the shear and permanent deformation properties of cold in-place recycled mixtures with bitumen emulsion using triaxial tests, Constr. Build. Mater. 328 (2022), 127054, https://doi.org/10.1016/j.conbuildmat.2022.127054.
[31] A. Grilli, S. Raschia, D. Perraton, A. Carter, A. Rahmanbeiki, P. Kara De Maeijer, D. Lo Presti, G. Airey, C. Ogbo, E.V. Dave, G. Tebaldi, Experimental investigation on water loss and stiffness of CBTM using different RA sources, RILEM Book. 27 (2022) 11–17, https://doi.org/10.1007/978-3-030-46455-4_2.
[32] G. Flores, Optimization of cold mixtures with emulsion and high RAP content (Doctoral Dissertation), Universidad Politécnica de Madrid, 2019.
[33] D. Needham, Developments in bitumen emulsion mixtures for roads, University of Nottingham, 1996.
[34] B. Gómez-Meijide, Aplicación sostenible de residuos de construcción y demolición como árido reciclado de mezclas bituminosas en frío. Ph.D. Dissertation. Universidade da Coruña, 2015.
[35] P. Orosa, Mechanical behaviour of cold in-place recycled asphalt mixtures with bitumen emulsion. Effect of curing time on the response of rehabilitated pavement sections. Ph.D. Dissertation. Universidade da Coruña, 2022.
[36] AENOR (Spanish Association for Standardisation and Certification), UNE - EN 13286–7. Unbound and hydraulically bound mixtures - Part 7: Cyclic load triaxial test for unbound mixtures, In Spanish, Madrid, 2008.
[37] A.I. Khuri, Response Surface Methodology. Int. Encycl. Stat. Sci, Springer Berlin Heidelberg, Berlin, Heidelberg, 2011, pp. 1229–1231, https://doi.org/10.1007/978-3-642-04898-2_492.
[38] A. Usman, M. Hartadi Sutanto, M. Bin Napiah, N. Shehu Aliyu Yaro, Response surface methodology optimization in asphalt mixtures: a review, Response Surf. Methodol. Eng. Sci., IntechOpen (2021), https://doi.org/10.5772/intechopen.95994.
[39] C. Moro, V. Francioso, M. Velay-Lizancos, Nano-TiO2 effects on high temperature resistance of recycled mortars, J. Clean. Prod. 263 (2020), 121581, https://doi.org/10.1016/j.jclepro.2020.121581.
[40] A. María Rodríguez Pasandín, J. José Galán-Díaz, L. Manuel Sousa da Silva, P. Orosa Iglesias, I. Pérez Pérez, Comparison of accelerated laboratory curing and maturation under uncontrolled conditions of gravel emulsions using a nonlinear weighted least-squares predictive model, (2022). https://doi.org/10.1080/10298436.2022.2144309.